

UAV and AI for large-scale monitoring of the effects of climate change on mountain lake areas: the ACLIMO cross-border cooperation project

Original

UAV and AI for large-scale monitoring of the effects of climate change on mountain lake areas: the ACLIMO cross-border cooperation project / Matrone, F., Graziani, C., Spadaro, A., Hemmatianzadeh, S., Lingua, A.M.. - In: INTERNATIONAL ARCHIVES OF THE PHOTOGRAMMETRY, REMOTE SENSING AND SPATIAL INFORMATION SCIENCES. - ISSN 1682-1750. - 48:(2025), pp. 203-210. (UAV-g 2025 Uncrewed Aerial Vehicles in Geomatics Espoo (Fin) 10–12 September 2025) [10.5194/isprs-archives-XLVIII-2-W11-2025-203-2025].

Availability:

This version is available at: 11583/3012643 since: 2026-07-02T14:21:40Z

Publisher:

Copernicus Publications

Published

DOI:10.5194/isprs-archives-XLVIII-2-W11-2025-203-2025

Terms of use:

This article is made available under terms and conditions as specified in the corresponding bibliographic description in the repository

Publisher copyright

(Article begins on next page)

UAV and AI for large-scale monitoring of the effects of climate change on mountain lake areas: the ACLIMO cross-border cooperation project

Francesca Matrone¹, Chiara Graziani¹, Alessandra Spadaro¹, Saeed Hemmatianzadeh¹, Andrea Maria Lingua¹

¹ Department of Environment, Land and Infrastructure Engineering (DIATI), Politecnico di Torino, Corso Duca degli Abruzzi 24, 10129, Turin, Italy – (chiara.graziani, andrea.lingua, francesca.matrone, alessandra.spadaro)@polito.it
saeed.hemmatianzadeh@studenti.polito.it

Keywords: Climate change, monitoring, UAV, vegetation classification, shallow water bathymetry, GeoAI

Abstract

Studying the effects of climate change is essential to understanding the impact of human activities on the environment and to developing effective mitigation and adaptation strategies. This is the objective of the ACLIMO project, which applies a multi-sensor and multiscale approach to analyse the effects of climate change on a border alpine area and specific ecosystems. In this contribution, we focus on the large-scale objectives, analysing vegetation coverage around two alpine lakes (Lake Brocan and Lake Vej del Bouc) and their bathymetry. In particular, through automatic classification of drone imagery with an Object-Based Image Analysis (OBIA) workflow, five machine learning algorithms (Bayesian, Random Forest, Support Vector Machine, K-Nearest Neighbours, Decision Tree) were tested for automatic classification of vegetation. Field surveys were conducted to collect in situ vegetation data, providing ground-truth points for classification validation. In addition, bathymetric mapping was carried out using a USV (Uncrewed Surface Vessel) equipped with a single-beam echo sounder, serving as ground-truth for bathymetric models derived via Structure-from-Motion analysis of UAV images. This integrated and in-depth methodology enabled the generation of detailed land cover maps highlighting dominant vegetation species and accurate 3D bathymetric models, allowing for a comprehensive ecological assessment of this alpine environment under ongoing climate change conditions and establishing a starting point (to data) for future monitoring and change detection analyses.

1. Introduction

Studying the effects of climate change is essential to understanding the impact of human activities on the environment and developing effective mitigation and adaptation strategies. These changes negatively affect places with fragile climates and conditions, such as mountain areas. A thorough understanding can thus allow us to protect the communities and environments most vulnerable to the effects of global warming. This contribution describes the methodology developed for a multiscale study and monitoring of a part of the Italian northwest border alpine region.

The ACLIMO project arises from the collaboration between the Politecnico di Torino and APAM (Management Body of *Aree Protette Alpi Marittime* - protected areas Maritime Alps) within the France-Italy ALCOTRA (Alpi Latine COoperazione TRAnsfrontaliera) European 2021/2027 project, which involves several Italian-French parks and bodies such as the *Parc National du Mercantour*, *Parc National des Ecrins*, *Gran Paradiso National Park*, *Regional Natural Park of Alpi Liguri*. The objectives of this collaboration include the analysis of the impacts of climate change on the mountain regions of the Maritime Alps park, with particular attention to glaciers, forests, grasslands, peat bogs, wetlands and water resources (Mauro, 2015). Furthermore, the project aims to support environmental management through the study of risk and vulnerability conditions, as well as the prediction of possible future dynamic evolutions.

As mentioned, we performed a multiscale and multi-sensor analysis of this mountain area, but this contribution focuses on the large-scale monitoring process, which consists of UAV surveys of two alpine lakes. The aim is to establish an efficient and effective method for mapping alpine vegetation types and canopy land cover classes as derived from medium-resolution

Sentinel-2 data combined with high-resolution UAV multispectral data, whose classification has been performed with the application of artificial intelligence algorithms (Huang et al., 2021). From the UAV surveys, we also carried out a bathymetry analysis of lakes with a Structure-from-Motion methodology, validated by a USV (Uncrewed Surface Vessel) bathymetry survey. This multi-source, multi-resolution method is significant for alpine regions, where spatial heterogeneity and sparse in-situ measurements often restrict the application of traditional remote sensing techniques.

The output is a transferable approach to monitoring vulnerable alpine ecosystems.

2. Materials and methods

2.1 The ACLIMO project

The methodology of the ACLIMO project consists of a multi-platform, multi-sensor and multiscale approach on three different levels: small, medium and large scale, applying consolidated and robust algorithms for supporting monitoring and decision processes by APAM.

The small-scale analysis focuses on studying the trends and variations of snow and the vegetation coverage. For this purpose, satellite images from *Copernicus Land Monitoring Service* (CLMS), Landsat and Sentinel satellites are used, covering a period of 20-25 years on three months, in particular: *April* (maximum snow cover period according to the Regional Agency for Environmental Protection - ARPA), *June* (maximum vegetation bloom and maximum water level in lakes due to snowmelt peak), *August* (for analysing perennial and residual snowfields and water level at the end of the summer period). Spatial trends of land cover will then be compared with data from weather stations located inside APAM territory.

In the medium scale, the focus is on the vegetation, wetlands and glaciers/snow. Multispectral aerial orthophotos are used to create a land cover and land use map with a higher resolution than the *Corine Land Cover* dataset. The map was classified automatically and semi-automatically through artificial intelligence (AI) techniques, particularly deep learning (DL) algorithms.

Two lakes have been considered large-scale indicators of climate change (Chunqiao et al., 2014) since they can constitute an example for studying vegetation and water level change over the years. Bathymetry and drone surveys with RGB and multispectral sensors were carried out for both lakes. In this case, machine learning-based (ML) recognition of elements of interest has been carried out to generate classification maps. These maps and the proposed methodology should then be adopted by APAM to continue the monitoring phases in the next years. This is one of the main reasons for the choice of ML algorithms, to have a simple and user-friendly methodology to be applied also by non-expert users.

2.2 The case study

More specifically, the Maritime Alps are located in the West-South portion of the Alpine Arc, south of the Piedmont region, Italy, and they are protected by the Protected Areas of Maritime Alps (APAM) body. The overall protected territory extends over 38.290 hectares and involves 16 municipalities, and the altitude ranges from 645 to 3297 m a.s.l. The main activities in this area are tourism and energy production, with the presence of the biggest hydropower plant in Italy, Luigi Einaudi plant, which has three reservoirs in Piastra, Rovina and Chiotas lakes. The latter is particularly important since it is next to one of the two lakes of analysis (the Lake Brocan, Figure 1).

For the multiscale approach of the ACLIMO project, three areas of analysis were chosen (Figure 1):

- for the small scale, we considered the entire area managed by APAM, namely the Alpine arc from Val Varaita to Alpi Liguri, crossing a portion of the plain close to Cuneo (Figure 1 - red area).
- a single and smaller valley for the medium scale (Valle Gesso, Figure 1 - blue area).
- two alpine lakes for the large scale: Lake Brocan (2004 m a.s.l.) and Lake Vej del Bouc (2054 m a.s.l.) (Figure 1 - yellow points)

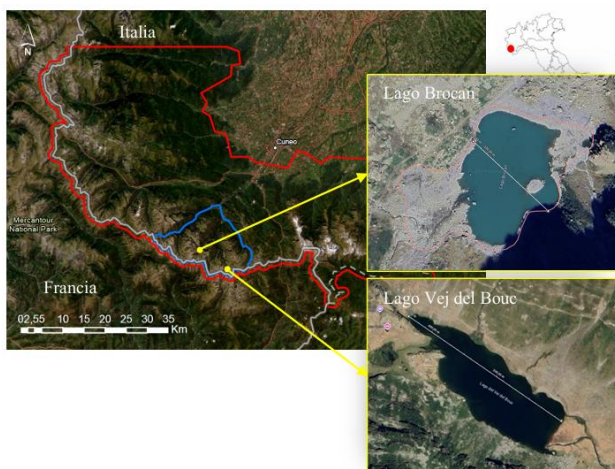


Figure 1. Surfaces of the areas of interest at the small scale (red), medium scale (blue) and large scale with lakes (yellow).

These two lakes were mainly chosen since Lake Brocan is characterised by a strong presence of anthropic activities, due to the hydropower plant, while Lake Vej del Bouc by pasture activities.

The vegetation of both lake basins is highly heterogeneous, comprising natural grasslands, mixed deciduous–conifer forests, and shrublands that differ in species abundance according to altitude, soil type, and available soil moisture. These plant assemblages are excellent indicators of environmental change and provide valuable information on alpine ecological mechanisms under climatic and anthropogenic stress.

As regards the bathymetry, the level of the two lakes is highly variable according to the year and, of course, season. For this reason, two survey campaigns are foreseen during the year: one during June-July and the other by September-October.

This contribution will mainly present the results of the large-scale analyses in which UAVs and USV have been involved.

2.3 Dataset

The UAV data acquisitions took place in July and October 2024. Two photogrammetric flights were carried out with DJI Mavic 3M (multispectral) and RTK module, for a total of 4947 images acquired for Lake Vej del Bouc and 6116 for Lake Brocan. The processing was carried out both with software DJI Terra and Agisoft Metashape, resulting in dense point clouds, as shown in Figure 2, with 28.083.475 points for Vej del Bouc and 32.467.868 points for Brocan, with RMSE of 2-3 cm (7 GCPs for lake Vej del Bouc and 10 GPCs for lake Brocan).

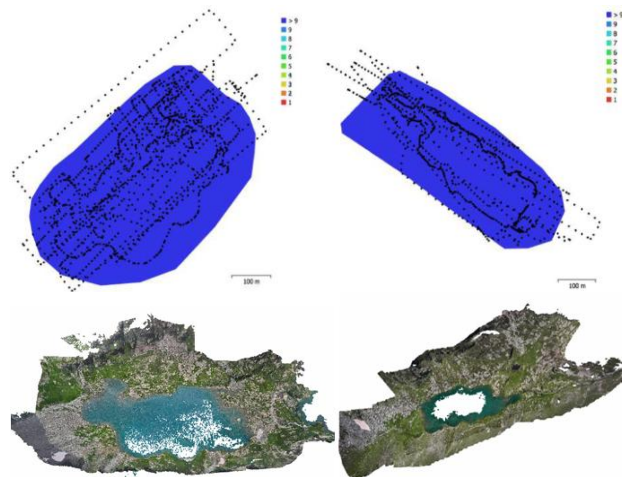


Figure 2. UAV images acquired and point clouds. Lake Brocan on the left, Lake Vej del Bouc on the right.

These point clouds were then processed to obtain orthophotos of the two lakes, used as a base for automatic vegetation classification.

Beyond high-resolution UAV-derived multispectral images, medium resolution Sentinel-2 MSI (Multispectral Instrument) data were also exploited for an initial large-scale analysis. The images have a 10 m resolution, providing a balance between detail and regional coverage. Images were obtained monthly, with a focus on the months of June, August, and September in the respective years. Twenty-four multispectral images were then chosen to represent the period from June 2017 to September 2023 and support multi-annual monitoring of vegetation and water-body trends.

Concerning the bathymetry, for the survey in Lake Vej del Bouc, the Alpha Wi STX-EchoS single-beam echo sounder was used. It was installed on the BlueBoat USV to collect data and transported in situ thanks to its small size (Table 1 and Figure 3). Table 1 resumes the instruments employed for in situ surveys and their characteristics:



Satellite	<p>Sentinel-2 Images from the months of April, June, and August (2017–2024) Spatial resolution: 10 m Spectral resolution: 13 bands</p>
UAV	<p>DJI Mavic 3M GNSS RTK, 5 sensors, RGB 4/3 (17.3 × 13 mm), 20 MP, 5280 × 3956, Pixel size: 3.3 × 3.3 μm Focal length: 13 mm, Multispectral 1/2.8", 6.058 × 4.415 mm, 5 MP, 2592 × 1944 Bands: Green (G): 560 ± 16 nm, Red (R): 650 ± 16 nm, Red Edge (RE): 730 ± 16 nm, Near-Infrared (NIR): 860 ± 26 nm Weight: 951 g</p> 
Bathymetry	<p>BlueBoat USV, Blue Robotics Maximum velocity 3 m/s, Weight 14,5 kg, Control length 250 m, Autonomy with 8 batteries: 62 hours</p>  <p>Echosounder STX-Echos Depth range 0.2 – 200 m, Resolution 8 mm, Acquisition angle 8° GNSS: GPS, GLONASS, BDS, GALILEO, QZSS Weight 1200 g</p>

Table 1. Sensors and dataset



Figure 3. BlueBoat USV, BlueRobotics, equipped with STX-Echos Echosounder (left); point acquisition on shallow water through GNSS receivers for validation (right).

3. Methodology for large-scale monitoring

The GNSS measuring of GCPs, UAVs surveys and USV surveys constitute an integrated system for analysing both the vegetation in the area of interest, generating land cover maps through automatic classification, and for reconstructing the bathymetry of water bodies from USV surveys and drones' images. Figure 4 shows the workflow of this study.

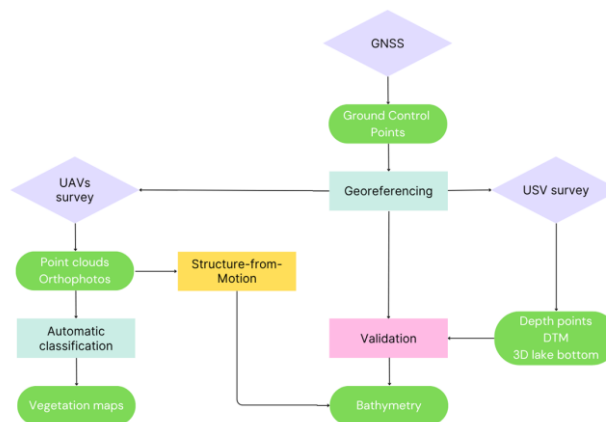


Figure 4. Methodological workflow.

3.1 Vegetation classification methodology

For the large-scale analysis with UAVs, a systemic approach was applied, including satellite imagery, UAV imagery, remote sensing indices, and state-of-the-art ML algorithms to classify alpine vegetation. In this way, a link between the small and medium scale analysis and the large scale one will be easily conducted in the project's next phases, allowing the identification of patterns, trends and effects of climate change.

3.1.1 Satellite data

The satellite-based part of this study was used as a coarse-resolution tool to monitor long-term changes in vegetation and water conditions over the two alpine lakes, Lake Brocan and Lake Vej del Bouc.

All pre-processing and analyses were conducted in Google Earth Engine (GEE): Sentinel-2 collections were sub-set by date, cloud cover, clipped spatially to the exact AOI extents, and quality was restored based on the QA60 band for cloud masking. For Level-1C products, atmospheric correction tasks in GEE were performed to normalise reflectance values and to cancel out atmospheric noise.

Following pre-processing, each of the images was resampled to an RGB composite and analysed for four important spectral indices that yield complementary information on surface conditions and ecological processes: NDVI (Normalised Difference Vegetation Index), NDWI (Normalised Difference Water Index), EVI (Enhanced Vegetation Index), and SAVI.

Land cover mapping was performed only with Random Forest (RF) in the Google Earth Engine (GEE) cloud computing platform. The criteria for this selection were the efficiency of the method in high-dimensional feature spaces and the robustness of the approach against overfitting. The training samples were manually digitised with reference to the UAV orthophotos and visual interpretation of Sentinel-2 scenes. Four major land cover types were classified, including open water, bare soil or rock, sparse, and dense vegetation.

The RF classifier was trained based on Sentinel-2 spectral bands and calculated indices as input features. The model was then applied in all the chosen scenes to produce consistent land cover maps at a 10-m interval. Classification products were exported from GEE as GeoTIFF and analysed in GIS for comparison and validation compared to UAV derived outputs.

3.1.2 UAVs imagery

The acquired images of the July and October UAV surveys carried out by Politecnico di Torino were elaborated with Agisoft Metashape. The orthophoto production was conducted independently for each of the five spectral bands (RGB, Red, Green, RedEdge, and NIR) with a photogrammetric processing at a high resolution (Figure 5 and 6). This was made to avoid co-registration error.

DSMs were also calculated from the dense clouds to represent changes in elevation of both vegetated and non-vegetated surfaces.

The so-produced multispectral orthophotos have been used as a base for automatic vegetation classification with eCognition software, through the object-based image analysis (OBIA) workflow. In order to increase the discriminative power of the classification, spectral indices NDVI and NDWI were calculated directly in eCognition with the help of the process tree module.

An initial multi-threshold segmentation was tried using index values to distinguish water, soil/rock, and vegetation. As the accuracy was not acceptable, the workflow was altered towards multi-resolution segmentation with customised weights per spectral band, resulting in a much-increased segmentation accuracy.

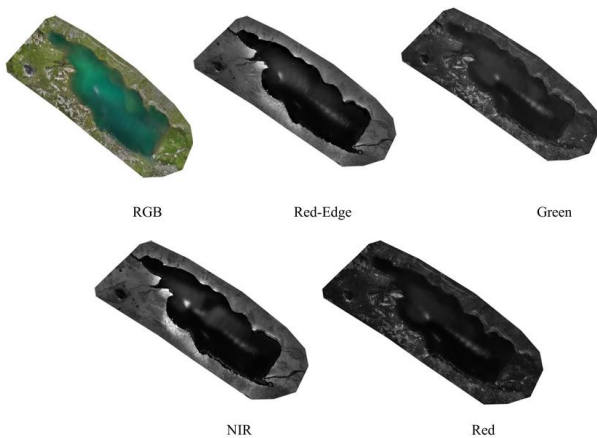


Figure 5. Five bands orthophotos for Lake Vej del Bouc

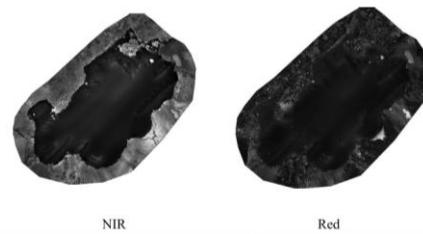
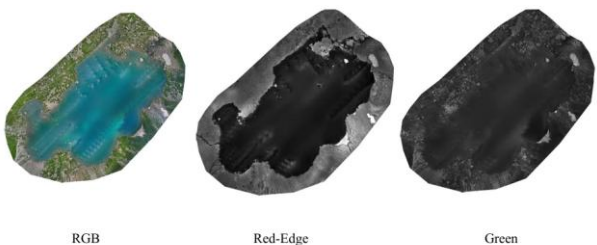


Figure 6. Five bands orthophotos for Lake Vej del Bouc

After obtaining the optimal segmentation, a large training set was created for the supervised classification. These samples spanned spectral variability across the lakes and in the surrounding terrain, which experienced shadow, variable vegetation coverage, and mixed pixels.

These samples were then subjected to five supervised machine-learning algorithms in eCognition: Bayesian, Support Vector Machine (SVM), K-Nearest Neighbors (KNN), Random Tree, and Random Forest. Each classifier was trained separately and operated independently, and classification performance was evaluated by matching outputs to known object classes and through visual validation.

After the overall land-cover classification (with general classes vegetation, rock/soil and water), a second classification step was implemented to obtain vegetation types. This second-level classification was performed on only the "vegetation class" derived from the first-step classification.

In addition, field activities and surveys on the shores of both lakes during in situ campaigns (Figure 7) served as ground-truth samples of the dominant plant species and vegetation clusters. These samples were used to determine the training set for vegetation sub-classes.





Figure 7. Definition of the ground truth for the species identification surveyed with GNSS receivers.

Table 2 shows the main vegetation species that were recorded with GNSS in the area of interest. These data and points were used to train the second-step algorithms.

Latin name	English name	Code
<i>Rumex Alpinus</i>	Alpine Dock	AD001
<i>Rumex Romice</i>	Sorrel	SO002
<i>Festula Rubra; o Festuca</i>	Red Fescue	RF003
<i>Trichophorum cespitosum</i>	Deergrass	DG004
<i>Carex nigra</i>	Black Sedge	BS006
<i>Nardus</i>	Matgrass	MG007
<i>Nardus Stricta</i>	Upright Matgrass	UM008
<i>Janiperus nana</i>	Dwarf Juniper	DJ009
<i>Rhododendron Ferrugineum</i>	Rusty-Leaf Rhododendron	RR010
<i>Festuca Paniculata</i>	Tussock Fescue	TF011
<i>Rubus Idaeus</i>	Red Raspberry	RI012
<i>Athurrium Filixoideas</i>	Lady Fern	AF013
<i>Dryopteris Flix-max</i>	Male Fern	DF014
<i>Vaccinium Mirtillus</i>	Bilberry	VM015
<i>Alnus Viridis</i>	Green Alder	AV016

Table 2. Vegetation types and codes.

3.2 Bathymetry methodology

3.2.1 USV Bathymetry

During the survey with the USV, 2972 points were acquired through a manual path (Figure 8a). The maximum registered depth is 8,59 m, at the centre of the lake. With MATLAB R2023a software, DTM and three-dimensional models of the bottom were recreated (Figure 8b) to be used as ground truth for the AI algorithms currently tested on the orthophotos.

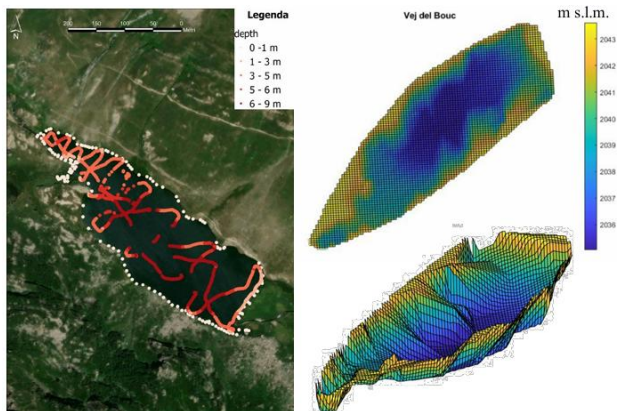


Figure 8. Lake Vej del Bouc: (left) points collected by the echo sounder; (right) reconstruction of the DTM with linear interpolation and 3D reconstruction of the lake bottom.

The generated 3D model of the lake bottom and the points acquired with the USV serve as ground truth for the validation of the bathymetry built with the Structure-from-Motion method on shallow water.

3.2.2 Bathymetry Structure-from-Motion

Bathymetry was calculated not only from the USV survey, but also through a Bathymetric Structure-from-Motion (SfM) methodology using the point cloud generated by UAVs survey (Dietrich, 2016). The main issue with this method is the refraction correction of light when it passes through two different media, air and water. This phenomenon underestimated the real depth of the water body, measuring a so called "apparent depth" (Figure 9).

To correct this error, an iterative algorithm is applied, which calculates a series of equations for the correction of the light refraction for every point/camera in the point cloud.

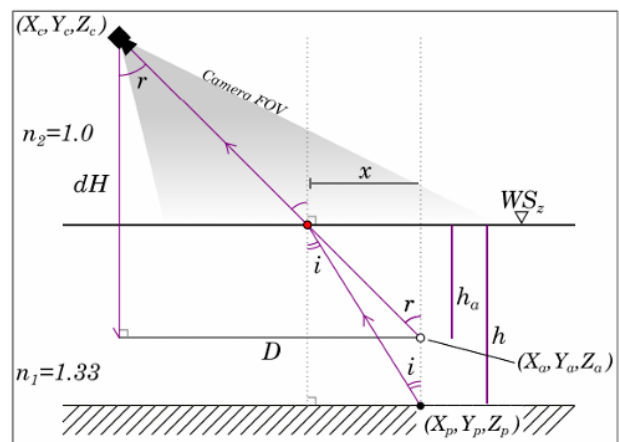


Figure 9. Trigonometry of the refraction. Variables are explained in Table 3:

Variables	Description
X_a, Y_a, Z_a	Apparent coordinates of SfM point
X_p, Y_p, Z_p	Real coordinates of the point
D	Euclidean distance between camera and SfM point
dH	Flight height over SfM point
r	Angle of refraction
i	Angle of incidence
x	Distance between SfM point and interface point water-air
h_a	Apparent depth of SfM point
h	Real depth of P point
n_1	Refractive index of water (1.337)
n_2	Refractive index of air (1.0)

Table 3. Description of variables in Figure 9.

The base equation is the Snell law, a formula used to describe the relationship between the angles of incidence and refraction, when referring to light or other waves passing through a boundary between two different isotropic media:

$$n_1 \sin i = n_2 \sin r \quad (1)$$

The aim is to solve a system of equations in order to define the effective depth, h .

Having different camera views for every point, it is very difficult to apply Snell law, since there are many cameras for each point and, as a result, different angles of incidence and of refraction and different apparent depth, h_a . This great quantity of values would create a noisy point cloud.

It is then necessary to apply this correction iteratively, for every combination point-camera, exploiting the trigonometry laws regarding refraction of light.

The first step is to test the visibility of points from all cameras to build the SfM cloud. This step has been carried out in Agisoft Metashape software. Once all visible points are found, the refraction angle is calculated as follows:

$$r = \tan^{-1} \frac{D}{dH} \quad (2)$$

The apparent depth is calculated as:

$$h_a = WS_z - Z_a \quad (3)$$

Once we know r and h_a , there are other variables to be computed in order to define h :

$$i = \sin^{-1} \left(\frac{n_1 \sin r}{n_2} \right) \quad (4)$$

$$x = h_a \tan r \quad (5)$$

$$h = \frac{x}{\tan i} \quad (6)$$

$$Z_p = WS_z - \tilde{h} \quad (7)$$

The corrected value of Z_p is given as the mean of all values of the real depth. It is subtracted by the surface of the water in order to obtain the real elevation, since our goal is to correct the DTM of lakes.

The surface of the water is obtained by the Kriging interpolation with the DTM of a series of points along the border of the lake.

For our purposes, we applied a Python `py_sfm_depth` algorithm (1). This Python script requires three .csv input files:

- Dense Cloud File, containing the point cloud to be corrected with coordinates, the SfM bathymetric height and the height of the surface water.
- Camera File, with the coordinates and orientation parameters (pitch, roll, yaw) of cameras in the same reference system.
- Sensor File, with the focal length of the camera and the physical dimensions of the sensor, both in millimeters.

Before applying the algorithm, it is necessary to define the area of interest and to create the shapefile containing only the points of the reservoir where water flows.

The output is a .csv file containing the planimetric coordinates, the geodetic height to be corrected, the surface water level, the apparent depth, the mean corrected depth and, with the subtraction of the water level, we finally obtain the correct geodetic height for each point.

4. Initial results

4.1 UAV imagery vegetation classification

The classification with Random Forest algorithm of satellite images gives back classification maps with three land cover classes: open water, vegetation, bare soil/rock (Figure 10). They were validated by reference data based on the UAV images: the Random Forest model provided classification accuracies of 85 to 92%, depending on the year and cloudiness.

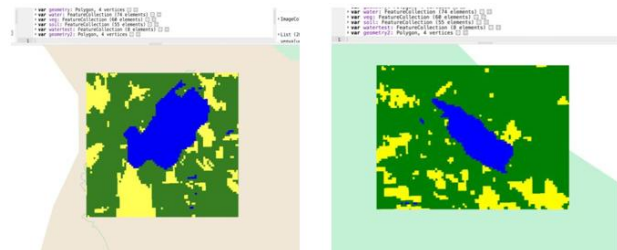


Figure 10. Random Forest classification in GEE

The post-classification change detection indicated that there has been a gradual reduction in the extent of dense vegetation cover, particularly at the edges of those on upper slopes. Reduced lake extents were seen in the most arid years (e.g., 2022) and were combined with declines of the NDWI. Vegetation belts seemed to rise, most likely in response to glacial retreat and the warmer climate developing.

The output produced after OBIA classification of UAVs imagery was exported and compared among classifiers. The highest classification accuracy was obtained using the Bayesian classifier, particularly for spectral separation of similar types of vegetation in complex terrain.

What we obtain is a high-resolution classification map of the typical alpine vegetation of this area (Figure 11).

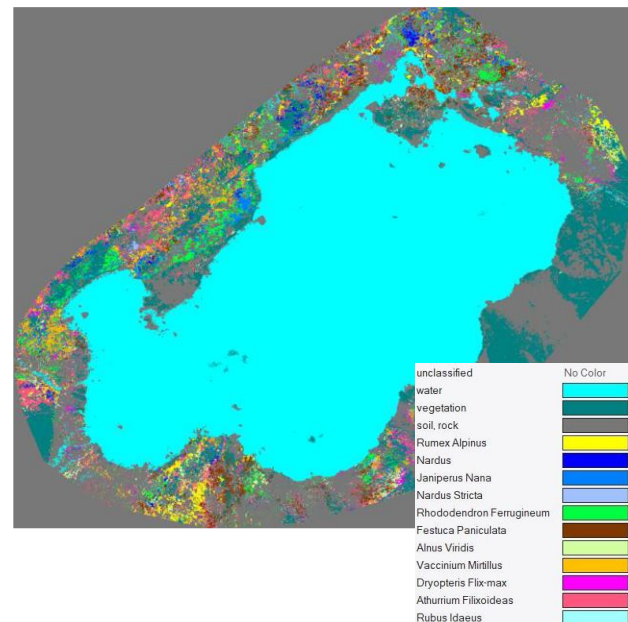


Figure 11. Automatic classification of vegetation for the Lake Brocan, Bayesian algorithm.

(2) https://github.com/geojames/py_sfm_depth

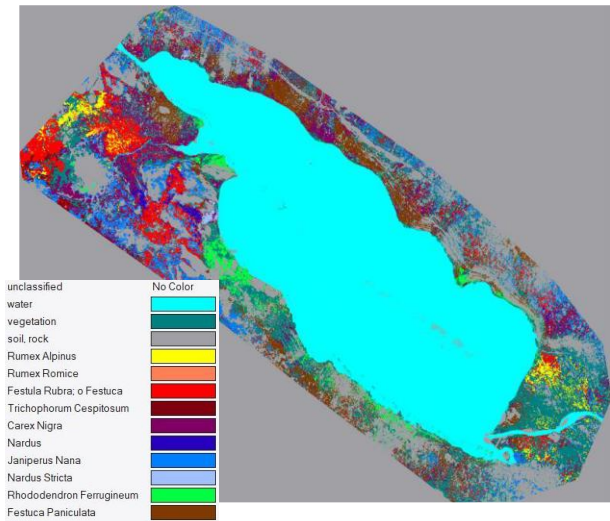


Figure 12. Automatic classification of vegetation for the Lake Vej del Bouc, Bayesian algorithm.

4.2 Bathymetry for shallow water

As explained in 3.2.2, the first step was to identify only those reconstructed points of the SfM point cloud where there was water (Figure 12).

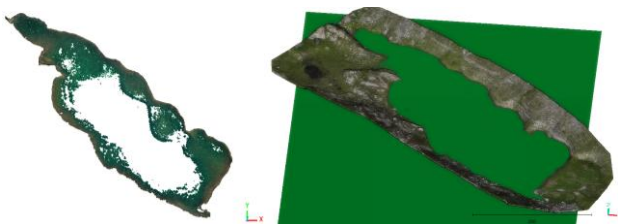


Figure 13. Point cloud of Lake Vej del Bouc, water only (left) and intersect plane for water surface (right).

This part is the only one of the SfM point cloud that is corrected by the algorithm; in particular, the point belonging to the shallow water class. Figure 14 shows the section (a) and the profile (b) of the original and the corrected point clouds with the real value for the geodetic height (marked in blue).

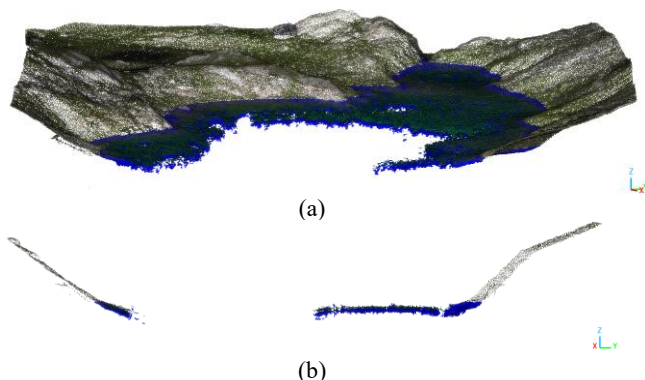


Figure 14. Section (a) and profile (b) of the corrected point cloud, Lake Vej del Bouc.

The corrected points highlight displacements of less than 10 cm for the points next to the lake shore, while higher values from 80 cm to 1,5 m for the points towards the centre of the lake (Figure 14).

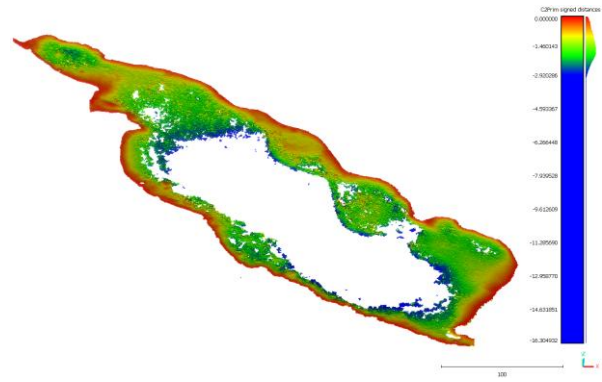


Figure 15. Cloud-to-cloud between the UAV SfM point cloud and the corrected one.

5. Discussions

5.1 UAV imagery classification

This investigation demonstrates the feasibility of multi-source object-based classification in alpine vegetation and land cover mapping from UAV images processed with GeoAI (Geospatial AI) algorithms. With the combination of medium-resolution Sentinel-2 satellite images and ultra-high-resolution UAV orthophotos, we succeeded in meeting the spatial dimensions of ecological monitoring in mountainous areas, while for the temporal one, new time series will be collected this year and in the future.

The integration of GEE for long-term processing of satellite data together with eCognition Developer for fine-scale classification of UAV-derived data enabled the achievement of a complete framework for the environment of the Maritime Alps. For satellite images classification, we registered overall classification accuracy rates between 85% and 92%, depending on the year and cloudiness; then compared with UAV-based orthophotos. For UAV imagery classification, among the five ML classifiers exploited, Bayesian algorithm performed best, all yielding accuracies over 94% (Figure 14). Its performance was especially strong in complex terrain or for spectral discrimination of vegetation classes that are spectrally similar, such as transient grassland types or mixed sedge communities. This is likely due to the probabilistic nature of the Bayesian model, which handles class uncertainty and overlapping spectral features more effectively than ensemble or kernel-based techniques.

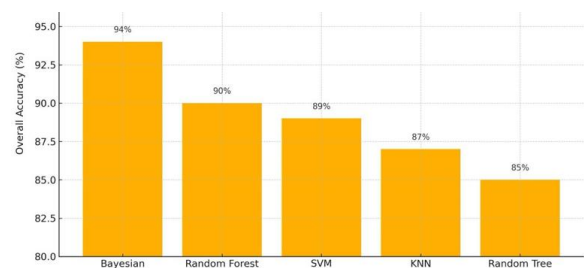


Figure 15. Comparison of accuracies among ML classifiers for the UAV fist-step classification (vegetation, soil, water).

Although in general the UAV workflow performed well, some problems occurred during data acquisition and processing. In a few of the north-facing or steeper slopes, shading led to underestimation of vegetation reflectance, with the consequence

of mistakenly assigning forested areas as exposed soil or even open water. In addition, some specific parts of the orthophoto mosaic (particularly in the area close to Lake Brocan) had visually degraded quality, possibly due to suboptimal flying conditions. Motion blur caused by wind-induced instability during data acquisition could have limited the quality of the final orthoimages, and on a few strips, the overlap between the images was lower than expected, weakening Metashape's ability to produce clean, radiometrically consistent products.

Apart from the orthophoto quality, co-registering spectral bands errors were present in several images, leading to a certain amount of misalignment that could have decreased classification accuracy at object edges.

Also of vital importance was the limited availability of ground-truth data. Field validation in the two lakes was restricted to specific zones around both sites because of the rough terrain, the presence of snow cover, and limited accessibility.

For the future, we intend to continue the in-situ surveys with the operators of APAM, who are currently validating the preliminary results of vegetation classification in order to improve the results and correct the misclassified elements. For the classification, we are going to implement topographic correction methods or shadow-invariant spectral indices to better discriminate classes.

5.2 Bathymetry

The result of the Python script for the correction of the depth is currently under validation with points registered with GNSS and USV during the surveys carried out in July (Figure 8).

The comparison between the SfM cloud and the corrected one allowed to observe the variance between the two datasets in the order of decimetres. There were some limits in using the Python algorithm, particularly in the requested parameters. In fact, the script works well in good atmospheric conditions, with limpid water and minimal superficial waves, so as the flight must respect some requisites, such as the use of a polarised filter, to keep the sun behind the sensor, to survey during the day to reduce shadows, and to acquire images with adequate overlapping, convergence and with slanting angles.

There were also some problems in acquiring images of the water surface from UAVs surveys, especially for higher depths, as we observed from point clouds (Figure 2). To reconstruct the orthophoto for Lake Brocan, patterns from shallow water were repeated in the central part of the lake.

Looking ahead, the integration of AI methods for correcting refraction errors in SfM-derived bathymetric models will be carried out, representing a promising direction to enhance depth estimation accuracy, especially in turbid and variable light conditions. Machine learning algorithms can be trained on combined SfM and sonar-derived datasets to learn systematic underestimations and compensate for them, as demonstrated in recent studies (Agrafiotis et al., 2019). This approach could reduce dependence on strict acquisition conditions and improve the replicability of UAV-based bathymetric surveys across different lake morphologies and environmental contexts, especially in the mountain ones where the transportation of heavy sensors and instruments as the USV could be difficult.

6. Conclusions

This study demonstrated the effectiveness of a multiscale, multi-sensor, and ML-based approach to set up the starting point (to data) for monitoring climate change impacts in alpine lake environments, with a focus on vegetation dynamics and

bathymetric reconstruction. The integration of high-resolution UAV multispectral imagery with medium-resolution satellite data enabled the production of detailed vegetation maps, essential for understanding local ecological processes in highly heterogeneous alpine regions. The application of object-based classification workflows and the testing of multiple ML classifiers highlighted the potential of Bayesian methods in achieving high classification accuracies, even in complex environments and under challenging illumination conditions. The bathymetric analysis using UAV-derived SfM methods, combined with USV surveys, will provide a replicable workflow for the generation of 3D lake bottom models, despite current limitations due to water refraction effects.

Future developments will focus on enhancing bathymetric accuracy using AI models to correct systematic depth underestimations and on refining vegetation mapping through the experts' validation. This integrated approach is a scalable and transferable method that can support protected area management in monitoring sensitive mountain ecosystems, contributing valuable data for climate adaptation strategies and sustainable management of alpine water resources.

Acknowledgement

The data has been acquired in collaboration with the operators of APAM (Aree Protette Alpi Marittime, *Protected Areas of Maritime Alps*) who supported the surveying campaigns.

The study is also partially funded by the project FAIR - Future Artificial Intelligence Research and received funding from the European Union Next-Generation EU (PIANO NAZIONALE DI RIPRESA E RESILIENZA (PNRR FAIR, CUP n. E13C22001800001) – MISSIONE 4 COMPONENTE 2, INVESTIMENTO 1.3 – D.D. 1555 11/10/2022, PE00000013). This manuscript reflects only the authors' views and opinions; neither the European Union nor the European Commission can be considered responsible for them.

The authors would also like to acknowledge master's Engineering student Daniel Felipe Cardozo Diaz for the preliminary bathymetry tests.

References

- Agrafiotis, P., Skarlatos D., Georgopoulos A., Karantzas K., 2019: Shallow water bathymetry mapping from UAV imagery based on machine learning. *The International Archives of the Photogrammetry, Remote Sensing and Spatial Information Sciences*. <https://doi.org/10.5194/isprs-archives-XLII-2-W10-9-2019>
- Chunqiao S., Bo H., Linghong K., Keith S. R., 2014: Remote sensing of alpine lake water environment changes on the Tibetan Plateau and surroundings: A review. *ISPRS Journal of Photogrammetry and Remote Sensing*, Volume 92.
- Dietrich, J. T., 2016: Bathymetric Structure-from-Motion: extracting shallow stream bathymetry from multi-view stereo photogrammetry. *John Wiley & Sons, Ltd*.
- Huang, H., Zhang, L., & Gong, W., 2021: Integrating UAV and machine learning for vegetation mapping in high relief mountain areas. *Remote Sensing*, 13(3), 401. <https://doi.org/10.3390/rs13030401>
- Mauro, G., 2015: Cambiamenti Climatici e Foreste Nell'Area Alpina: Telerilevamento a Bassa Risoluzione Spaziale per il Monitoraggio Della Vegetazione Boschiva. *Archivio per l'Alto Adige*, 108/109, pp. 145-165.